nature immunology

Different routes of bacterial infection induce long-lived T_H1 memory cells and short-lived T_H17 cells

Marion Pepper[1,2], Jonathan L Linehan[1,2], Antonio J Pagán[1], Traci Zell[1], Thamotharampillai Dileepan[1], P Patrick Cleary[1] & Marc K Jenkins[1]

We used a sensitive method based on tetramers of peptide and major histocompatibility complex II (pMHCII) to determine whether CD4+ memory T cells resemble the T helper type 1 (T_H1) and interleukin 17 (IL-17)-producing T helper (T_H17) subsets described *in vitro*. Intravenous or intranasal infection with *Listeria monocytogenes* induced pMHCII-specific CD4+ naive T cells to proliferate and produce effector cells, about 10% of which resembled T_H1 or T_H17 cells, respectively. T_H1 cells were also present among the memory cells that survived 3 months after infection, whereas T_H17 cells disappeared. The short lifespan of T_H17 cells was associated with small amounts of the antiapoptotic protein Bcl-2, the IL-15 receptor and the receptor CD27, and little homeostatic proliferation. These results suggest that T_H1 cells induced by intravenous infection are more efficient at entering the memory pool than are T_H17 cells induced by intranasal infection.

© 2010 Nature America, Inc. All rights reserved.

Vaccination or prior encounter with a microbe generally results in immunity to subsequent infection with that microbe. This immunity is mediated by memory T cells and B cells, which are generated from naive precursor cells after exposure to microbial antigens. Binding of the T cell antigen receptor (TCR) to microbe-derived peptide bound to major histocompatibility complex molecules (pMHC) causes naive T cells to proliferate and to differentiate into effector cells able to produce microbicidal cytokines[1]. Although ~90% of the effector cells die, some survive to become long-lived memory cells capable of a rapid and protective response to reinfection with the relevant microbe[2].

Two main subsets of memory T cells have been described: central memory T cells (T_{CM} cells) and effector memory T cells (T_{EM} cells)[3–5]. T_{CM} cells express the chemokine receptor CCR7 (A000630) and L-selectin, which allows recirculation through lymph nodes. T_{EM} cells lack CCR7 and L-selectin yet express other homing receptors needed for migration into nonlymphoid organs[6]. When stimulated with antigen, T_{EM} cells are immediately capable of effector cytokine production and cytolysis, whereas T_{CM} cells proliferate to produce new effector cells, which then acquire these functions. Heterogeneity in lymphokine production potential also exists in the case of CD4+ T cells. Naive CD4+ T cells differentiate into T helper type 1 (T_H1), T_H2 or interleukin 17 (IL-17)-producing T helper (T_H17) effector cells when stimulated *in vitro* with antigen and specific combinations of cytokines[7]. In addition, certain infections induce CD4+ effector cells with the properties of T_H1 or T_H2 cells[8].

However, it is still not clear that CD4+ memory T cells specific for peptide–MHC class II (pMHCII) exist as discrete T_H1, T_H2 or T_H17 subsets *in vivo* because such cells are difficult to detect in normal hosts. To circumvent this problem, researchers have studied immune memory by CD4+ T cells *in vitro*[9], or *in vivo*[1,10,11] by adoptive transfer of TCR-transgenic T cells. These approaches are artificial in that memory T cells are generated from disrupted lymphoid tissue[9–11] or are so abundant that normal homeostasis is perturbed[12–14]. Thus, it is not clear how well polyclonal CD4+ memory T cells fit into the T_H1, T_H2, T_H17 or T_{CM} and T_{EM} categories.

Here we addressed this problem with a sensitive pMHCII tetramer–based approach that allowed detection of polyclonal pMHCII-specific CD4+ T cells in normal mice after infection with *Listeria monocytogenes*. We found that intravenous and intranasal infection induced T_H1 and T_H17 CD4+ effector T cells, respectively, although the most abundant cells in both cases did not resemble any of the canonical helper T cell subsets. In addition, we found that T_H1 cells were much more likely than T_H17 cells to enter the memory cell pool.

RESULTS

Detection of pMHCII-specific CD4+ memory T cells

We used a pMHCII tetramer–based approach to identify CD4+ T cells specific for a pMHCII complex produced during bacterial infection. The pMHCII tetramer consisted of the I-A^b MHC class II molecule bound to a variant of amino acids 52–68 from the I-E α-chain called 2W1S (2W1S:I-A^b)[15]. The 2W1S peptide is highly immunogenic in C57BL/6 (B6) mice because of a relatively large naive population able to recognize 2W1S:I-A^b (ref. 16). We infected B6 mice with an attenuated strain of *L. monocytogenes* (ΔActA) engineered to secrete a fusion protein containing a portion of chicken ovalbumin and the 2W1S peptide (LM-2W1S)[17] or the mycobacterial peptide ESAT6 (LM-ESAT6)[18]. These bacteria replicate for several days in mice and are then completely eliminated by innate and adaptive

[1]Department of Microbiology, Center for Immunology, University of Minnesota Medical School, Minneapolis, Minnesota, USA. [2]These authors contributed equally to this work. Correspondence should be addressed to M.K.J. (jenki002@umn.edu).

Received 7 May; accepted 19 October; published online 22 November 2009; doi:10.1038/ni.1826

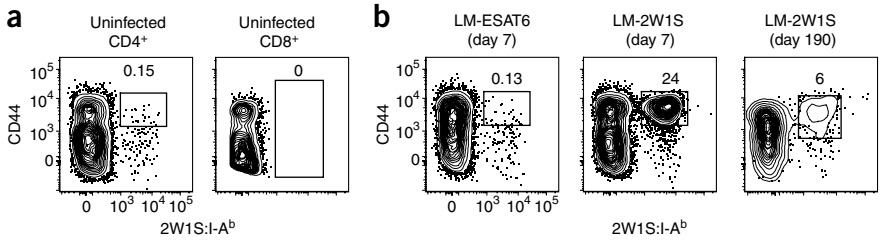


Figure 1 Infection with LM-2W1S induces the clonal expansion of 2W1S:I-A^b–specific memory cells. Flow cytometry to identify $CD4^+$ or $CD8^+$ T cells in enriched fractions, for events gated on $CD11c^-CD11b^-F4/80^-B220^-CD3^+$ cells. (**a**) $CD4^+$ T cells (left) or $CD8^+$ T cells (right) from an uninfected B6 mouse, gated on $CD44^{hi}$ 2W1S:I-A^{b+} cells (left) or all 2W1S:I-A^{b+} cells (right). (**b**) $CD4^+$ T cells in enriched samples from a B6 mouse 7 d after intravenous infection with LM-ESAT6 (left) or 7 d (middle) or 190 d (right) after intravenous infection with LM-2W1S. Numbers above outlined areas indicate percent cells in gate. Data are representative of over twenty (**a**) or two to five (**b**) independent experiments.

immune mechanisms[19]. We stained cells from each mouse with a fluorochrome-labeled 2W1S:I-A^b tetramer and anti-fluorochrome magnetic beads at various times after infection and enriched them on a magnetized column[20]. We then stained the bound fraction with antibodies specific for CD3, CD4, CD8 and CD44 and a 'cocktail' of non–T cell lineage–specific antibodies to aid in the identification of $CD4^+$ memory T cells.

Because effector and memory T cells express many of the same surface markers, we identified the latter cells as the population that stabilized after the expansion and contraction phases of the primary response[21]. Our initial analyses involved standard intravenous infection. Mice that were not infected contained a small population of about 300 2W1S:I-A^b–binding $CD3^+CD4^+$ cells in the spleen and lymph nodes, the vast majority of which were $CD44^{lo}$, as expected for naive cells (**Fig. 1a**). The tetramer bound to these T cells via the TCR, as shown by the finding that we detected no 2W1S:I-A^b–binding cells among the $CD8^+$ MHC class I–restricted T cells. Mice infected 7 d earlier with LM-ESAT6 also contained about 300 $CD44^{lo}$ 2W1S:I-A^{b+} $CD4^+$ naive T cells (**Fig. 1b**). In contrast, mice infected with LM-2W1S 7 d earlier contained a large population of $CD44^{hi}$ 2W1S:I-A^{b+} $CD4^+$ T cells in the spleen and lymph nodes that could still be detected on day 190 and beyond. The number of 2W1S:I-A^b–specific $CD4^+$ T cells peaked at ~140,000 cells by day 5 after LM-2W1S infection and then decreased rapidly to 20,000 cells by day 20 (**Fig. 2**). This contraction phase ended abruptly on day 20, after which the population slowly decreased until day 250, with a half-life of about 40 d (**Fig. 2**). By day 250, only about 200 $CD44^{hi}$ 2W1S:I-A^{b+} $CD4^+$ T cells remained in the spleen and lymph nodes, and this number remained stable for the next 150 d. Although we did not detect 2W1S:I-A^{b+} $CD4^+$ T cells in the bone marrow in uninfected mice (data not shown), about 1,500 $CD44^{hi}$ 2W1S:I-A^{b+} $CD4^+$ T cells appeared in the bone marrow by day 20 and then decreased to 150 cells by day 300. Thus, 2W1S:I-A^b–specific $CD4^+$ T cell populations expanded to a peak number on day 5, contracted until day 20, and then entered a memory phase characterized by slow numerical decrease for the next 230 d. In addition, some of the 2W1S:I-A^b–specific memory $CD4^+$ T cells were present in the bone marrow, although more were present in the spleen and lymph nodes.

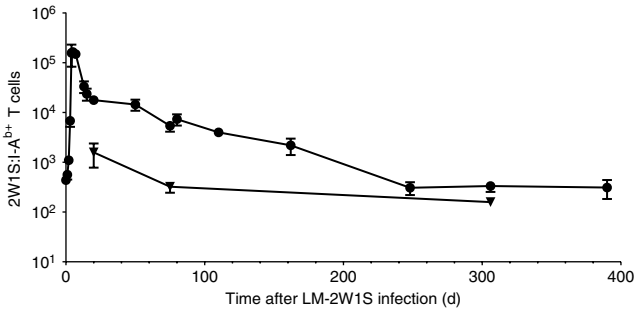


Figure 2 The 2W1S:I-A^b–specific $CD4^+$ memory T cells decay after infection with LM-2W1S. $CD4^+$ 2W1S:I-A^{b+} T cells in the spleen and lymph nodes (circles) or bone marrow (triangles) after intravenous infection of LM-2W1S ($n \geq 3$ mice per data point). A nonlinear regression fit of the spleen and lymph node data yielded a half-life of 43 d for points between days 20 and 248 ($R^2 = 0.94$; 95% confidence interval, 30–73 d). Data are representative of five experiments (mean ± s.e.m.).

Infection route influences $CD4^+$ T cell differentiation

We next determined whether $CD4^+$ memory cells induced by intravenous infection resembled any of the canonical helper T cell subsets. We measured lymphokine production by 2W1S:I-A^b–specific $CD4^+$ memory cells by direct *ex vivo* intracellular staining[22] in mice that were infected 24 d before with LM-2W1S and then challenged for 2 h with LM-2W1S or LM-ESAT6. We chose 2 h because this is the time of maximal *in vivo* lymphokine production by antigen-experienced $CD4^+$ T cells stimulated by intravenous injection of peptide[23] or infection with LM-2W1S (data not shown). We found that 2W1S:I-A^b–specific $CD4^+$ memory cells did not express CD69 (**Fig. 3a**) or produce interferon-γ (IFN-γ) or IL-17A after challenge with LM-ESAT6 (**Fig. 3a**,**b**). In contrast, about 30–40% of the memory cells produced IFN-γ after challenge with LM-2W1S (**Fig. 3a**,**b**), whereas none of these cells produced IL-17A (**Fig. 3b**) or IL-5 (data not shown). The failure of the majority of 2W1S:I-A^b–specific $CD4^+$ memory cells to make IFN-γ after challenge was not related solely to a lack of 2W1S:I-A^b recognition after challenge, as many of the cells expressed the TCR signal–dependent CD69 molecule but did not make IFN-γ (**Fig. 3a**). Therefore, about one third of the 2W1S:I-A^b–specific $CD4^+$ memory cells induced by intravenous infection resembled T_H1 cells, whereas the remainder did not produce any of the canonical T_H1, T_H2 or T_H17 cytokines.

It was possible that many of the 2W1S:I-A^b–specific $CD4^+$ memory cells that were $CD69^+$ but were not making cytokines 2 h after challenge would have gone on to produce cytokines. To address this issue, we stimulated spleen and lymph node cells from mice infected 22 d earlier with LM-2W1S *in vitro* with the soluble TCR signal mimics phorbol 12-myristate 13-acetate and ionomycin in the presence of an exocytosis inhibitor. IFN-γ-producing cells peaked at about 50% of the total 2W1S:I-A^b-specific $CD4^+$ memory population between 3.5 and 6 h of stimulation (**Fig. 3c**). As IFN-γ should accumulate in these conditions, these results indicated that only a subset of the 2W1S:I-A^b–specific $CD4^+$ memory cell population had the potential to produce IFN-γ. This conclusion was supported by the finding that about 50% of the 2W1S:I-A^b–specific $CD4^+$ memory cells induced by intravenous infection expressed the T_H1-associated transcription factor T-bet[24] before challenge, whereas none expressed

© 2010 Nature America, Inc. All rights reserved.

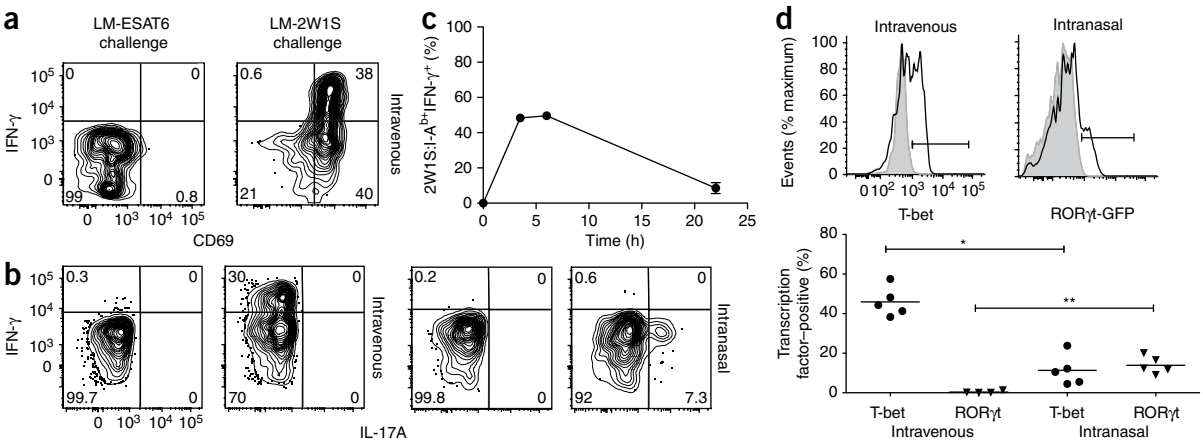


Figure 3 Lymphokine production by 2W1S:I-A^b–specific CD4$^+$ memory T cells. (**a**,**b**) Expression of CD69 (**a**) or IFN-γ (**a**,**b**) and IL-17A production (**b**) by 2W1S:I-A^b–specific memory T cells induced by intravenous (**a**,**b**) or intranasal (**b**) infection and challenged for 2 h with LM-ESAT6 (left) or LM-2W1S (right). Numbers in quadrants indicate percent cells in each. (**c**) Frequency of 2W1S:I-A^b–specific IFN-γ$^+$ CD4$^+$ memory T cells after stimulation for 3.5, 6 or 22 h with phorbol 12-myristate 13-acetate and ionomycin in the presence of brefeldin A. (**d**) T-bet expression (top left) in 2W1S:I-A^b–specific memory T cells (black line) induced by intravenous infection and in CD44$^+$CD4$^+$ T-bet-deficient cells (gray-filled histogram), and expression of enhanced green fluorescent protein (top right) in mice heterozygous for green fluorescent protein–tagged RORγt (RORγt-GFP) in 2W1S:I-A^b–specific memory T cells (black line) and naive 2W1S:I-A^b–CD44^{lo} T cells (gray-filled histogram) after intranasal infection. Below, frequency of T-bet$^+$ or RORγt$^+$ 2W1S:I-A^b–specific memory T cells in mice based on the gates above. $*P < 0.01$, T-bet samples, and $**P < 0.05$, RORγt samples (one-way analysis of variance with Bonferroni's post-test). Data are representative of three (**a**), six (**b**) or two (**c**) independent experiments, or of four or one independent experiment(s) for intracellular staining or heterozygous RORγt-GFP mice, respectively (**d**).

the T$_H$17-associated transcription factor RORγt[25] (**Fig. 3d**) and none became Foxp3$^+$ regulatory T cells[17]. As T-bet expression controls the T$_H$1 differentiation program in most cases[24], this finding indicated that only a subset of the memory cells induced by intravenous infection had differentiated into T$_H$1 cells.

One factor potentially driving the induction of T$_H$1 but not that of T$_H$17 or T$_H$2 cells was the intravenous route of infection. We therefore studied the effect of intranasal administration of LM-2W1S based on reports that IL-17A-producing T cells are induced during mucosal bacterial infection[26,27]. Indeed, we found that about 7% of the 2W1S:I-A^b–specific CD4$^+$ T cells in the spleen and lymph nodes of mice 24 d after intranasal infection with LM-2W1S produced IL-17A, whereas very few produced IFN-γ, 2 h after challenge with LM-2W1S but not after challenge with LM-ESAT6 (**Fig. 3b**). In addition, about 15% of the 2W1S:I-A^b–specific T cells induced by intranasal infection expressed RORγt, as shown by the expression of green fluorescent protein in mice heterozygous for expression of green fluorescent protein–tagged RORγt and by intracellular staining for RORγt (**Fig. 3d**). These results demonstrate that intranasal infection with LM-2W1S induced some of the 2W1S:I-A^b–specific T cells to differentiate into T$_H$17 cells. However, as with intravenous infection, the main population showed no evidence of committing to either a T$_H$1 or T$_H$17 canonical lineage.

T$_H$17 cells are shorter-lived than T$_H$1 cells

We next measured the survival of IFN-γ- or IL-17A-producing T cells to determine if these subsets were equally efficient at entering the memory pool. We infected mice and then challenged them later at various times with an intravenous injection of LM-2W1S to identify the lymphokine-producing cells. Intravenous infection with LM-2W1S generated about 12,000 IFN-γ-producing 2W1S:I-A^b–specific effector T cells in the spleen and lymph nodes by day 7, which constituted about 10% of all 2W1S:I-A^b–specific T cells. At all times after the contraction phase, IFN-γ-producing cells accounted for about 25% of the 2W1S:I-A^b–specific memory cells (**Fig. 4a**). Therefore, IFN-γ-producing 2W1S:I-A^b–specific T cells were as good as or better than non-IFN-γ-producing cells at entering the memory pool.

Intranasal infection induced a pattern of 2W1S:I-A^b–specific CD4$^+$ T cell population expansion, contraction and memory cell formation similar to that induced by intravenous infection, albeit to a lower extent (**Fig. 4b**). The lower magnitude of this response was probably related to the fact that the nasal mucosal lymphoid tissues, which are the main sites of priming after intranasal infection[28], contain many fewer naive T cells than does the spleen, where priming occurs after intravenous infection. About 2,000 IL-17A-producing 2W1S:I-A^b–specific effector cells were present on day 7, which, as for IFN-γ-producing cells in intravenously infected mice, constituted about 10% of all 2W1S:I-A^b–specific T cells at this time. However, unlike IFN-γ-producing cells, IL-17A-producing 2W1S:I-A^b–specific cells were progressively lost, such that fewer than 10 cells (or 0.5% of all 2W1S:I-A^b–specific T cells) remained at day 110 after infection. Thus, IL-17A-producing cells did not enter the memory pool as efficiently as IFN-γ-producing cells did.

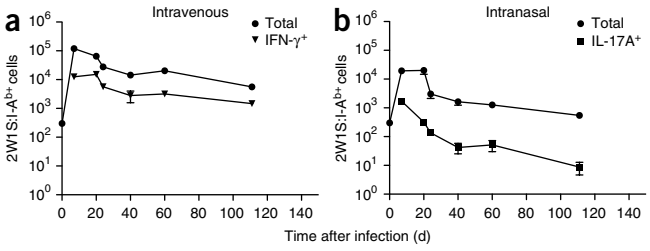


Figure 4 Survival of IFN-γ- and IL-17A-producing 2W1S:I-A^b–specific CD4$^+$ memory T cells. Total 2W1S:I-A^b–specific CD4$^+$ T cells induced by intravenous infection (**a**) or intranasal infection (**b**), and 2W1S:I-A^b–specific CD4$^+$ T cells making IFN-γ but not IL-17A (**a**) or IL-17A but not IFN-γ (**b**) after challenge with LM-2W1S. Data are representative of three (**a**) or two (**b**) experiments (mean ± s.e.m. of three to five mice per time point).

© 2010 Nature America, Inc. All rights reserved.

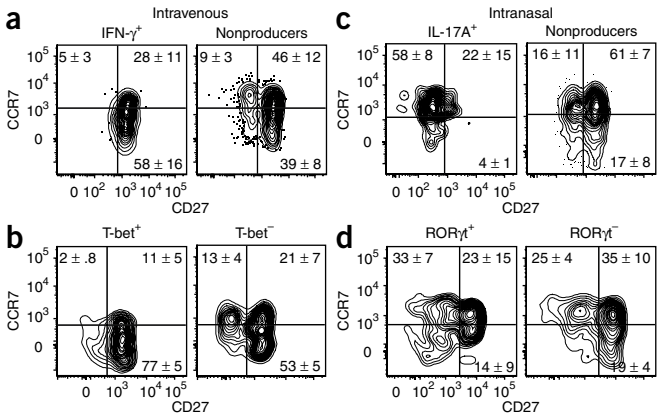


Figure 5 Surface phenotype of 2W1S:I-A^b–specific T cells. Expression of CCR7 and CD27 on 2W1S:I-A^b–specific T cells in mice at least 20 d after intravenous infection (**a**,**b**) or intranasal infection (**c**,**d**). (**a**) Cells producing IFN-γ but not IL-17A (left) or neither (right) after challenge with LM-2W1S. (**b**) T-bet$^+$ (left) or T-bet$^-$ (right) antigen-experienced cells without challenge. (**c**) Cells producing IL-17A but not IFN-γ (left) or neither (right) after challenge with LM-2W1S. (**d**) RORγt$^+$ (left) or RORγt$^-$ (right) antigen-experienced cells without challenge. Quadrant lines are based on 2W1S:I-A^b–CD44^{lo} naive cells in each sample; this population was uniformly CCR7^{hi} and contained CD27^{lo} and CD27^{hi} subsets. Horizontal lines are set at the smallest amount of CCR7 for the entire population; vertical lines are set at the midpoint between the CD27^{lo} and CD27^{hi} subsets. Numbers in quadrants indicate percent cells in each (mean ± s.d. of four or more mice). Data are representative of seven (**a**), four (**b**), six (**c**) or two (**d**) independent experiments.

CD27 marks functional heterogeneity in CD4$^+$ memory T cells

We sought additional markers that could give clues about the differences in the longevity of IFN-γ- and IL-17A-producing CD4$^+$ T cells and determine if they resembled T_{CM} cells or T_{EM} cells. Published work has demonstrated that CD8$^+$ memory T cells can be categorized on the basis of expression of the tumor necrosis factor receptor family member CD27 (A000546)[29,30]. In addition, CD8$^+$ memory cells that lack expression of CD27 have been shown to be short-lived[30–33]. Therefore, we assessed expression of CD27 and CCR7, a marker used to distinguish T_{CM} cells from T_{EM} cells[3]. Most of the IFN-γ$^+$ or T-bet$^+$ 2W1S:I-A^b–specific CD4$^+$ T cells present more than 20 d after intravenous infection were CCR7^{lo}CD27$^+$ (**Fig. 5a**,**b**). Although cells with this phenotype were also present among the IFN-γ$^-$ or T-bet$^-$ cells in the same mice, these populations also contained many CCR7^{hi}CD27$^+$ and CCR7^{hi}CD27$^-$ cells. In contrast, most of the IL-17A$^+$ 2W1S:I-A^b–specific CD4$^+$ T cells present after intranasal infection were CCR7^{hi}CD27$^-$ (**Fig. 5c**), whereas the IL-17A$^-$ cells included more CCR7^{hi}CD27$^+$ and CCR7^{hi}CD27$^-$ cells like the IFN-γ$^-$ cells in intravenously infected mice. Although the RORγt$^+$ 2W1S:I-A^b–specific CD4$^+$ T cells included CCR7^{hi}CD27$^-$ cells, as in the case of IL-17A-producing cells (**Fig. 5d**), the RORγt$^+$ populations also contained CD27$^+$ cells. Therefore, on the basis of CCR7 expression, the T_H1 cells resembled T_{EM} cells, whereas the T_H17 cells resembled T_{CM} cells.

The finding that IL-17A-producing CD4$^+$ T cells lacked CD27 and were short-lived motivated us to explore whether all CD27$^-$ CD4$^+$ memory cells had this property. We tested this possibility in an adoptive-transfer experiment involving total CD4$^+$ memory T cells, as 2W1S:I-A^b–specific memory cells were too infrequent to detect reliably after transfer. We sorted purified total CD27$^+$ or CD27$^-$ CD4$^+$CD44$^+$ T cells from *L. monocytogenes*–infected B6 mice (CD90.2$^+$) and transferred them into naive B6.PL-Thy-1^a (CD90.1$^+$) recipients (**Fig. 6a**). The CD27$^+$ CD4$^+$ memory cells survived stably over a 14-day period after adoptive transfer, whereas the number of purified CD27$^-$ CD4$^+$ memory cells decreased by about 80% (**Fig. 6b**). Thus, CD27$^-$ CD4$^+$ memory T cells were short-lived compared with CD27$^+$ CD4$^+$ memory T cells. Although this observation was based on total CD4$^+$ memory cells, it correlated with the finding that a subset of CD27$^+$ 2W1S:I-A^b–specific CD4$^+$ memory T cells expressed more of the survival protein Bcl-2 than did CD27$^-$ memory T cells of the same specificity (**Fig. 6c**).

Minimal homeostatic proliferation by CD27$^-$ CD4$^+$ T cells

It was also possible that poor homeostatic proliferation contributed to the short lifespan of CD27$^-$ CD4$^+$ memory T cells. We tested this possibility with a bromo-2-deoxyuridine (BrdU)-labeling experiment. We infected B6 mice with LM-2W1S and, 40 d later, gave the mice BrdU in their drinking water for 2 weeks. About 10% of the 2W1S:I-A^b–specific CD4$^+$ memory T cells induced by intravenous or intranasal infection labeled with BrdU (**Fig. 7a** and data not shown). Among the 2W1S:I-A^b–specific CD4$^+$ memory T cells, about 15% of the CD27$^+$ cells and only 3% of the CD27$^-$ cells labeled with BrdU (**Fig. 7a**,**b**). The homeostatic proliferation results correlated with expression of the β-chain of the IL-15 receptor (IL-15R; also known as CD122). CD122 was expressed on some CD27$^+$ CD4$^+$ memory T cells but very few CD27$^-$ CD4$^+$ memory T cells (**Fig. 7c**). Together, these results showed that CD27$^-$ CD4$^+$ memory T cells were poor homeostatic proliferators, perhaps as a result of a lack of IL-15R expression.

To further test that hypothesis, we injected mice with IL-15–IL-15Rα complexes, which have been shown to be superagonists for IL-15R signaling *in vivo*[34]. Injection of IL-15–IL-15Rα complexes into B6 mice 40 d after intravenous infection with LM-2W1S led to an increase of ~30-fold in the fraction of 2W1S:I-A^b–specific CD4$^+$ memory cells that underwent homeostatic proliferation over a short 5-day BrdU-labeling period, and the populations that proliferated were enriched for CD27$^+$ cells (**Fig. 7d**). These results

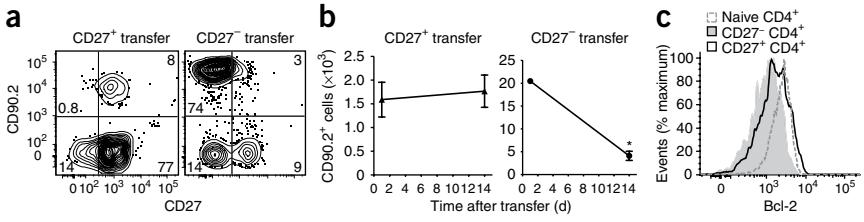


Figure 6 CD27$^-$ CD4$^+$ memory T cells are short-lived. (**a**) CD90.2-enriched fractions of spleen and lymph node cells from mice that received purified CD90.2$^+$ CD27$^+$ (left) or CD27$^-$ (right) total CD4$^+$ memory T cells 1 d earlier. (**b**) CD90.2$^+$ CD27$^+$ (left) or CD27$^-$ (right) cells recovered 1 or 14 d after transfer into B6.PL-Thy-1^a recipients. *$P = 0.0005$, CD27$^-$ cells recovered on day 14 versus day 1 (unpaired two-tailed Student's *t*-test). (**c**) Bcl-2 expression by total naive CD4$^+$ T cells (dashed line), or CD27$^-$ (gray-filled histogram) or CD27$^+$ (black line) 2W1S:I-A^{b+} memory T cells. Data are representative of three (**a**,**b**) or two (**c**) independent experiments (mean ± s.d. of three to four mice in **b**).

© 2010 Nature America, Inc. All rights reserved.

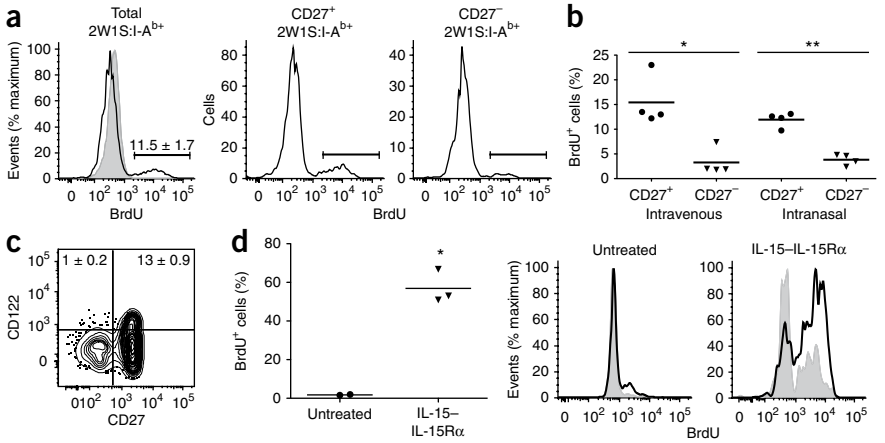


Figure 7 CD4$^+$ memory T cells undergo limited homeostatic proliferation. (**a**) BrdU labeling (black lines) of total (left), CD27$^+$ (middle) or CD27$^-$ (right) 2W1S:I-A^{b+} CD4$^+$ memory cells in mice fed BrdU for 14 d beginning 40 d after intravenous infection with LM-2W1S, as well as total CD4$^+$ T cells (gray-filled histogram) from a mouse that did not receive BrdU (left). Bracketed lines indicate gates used to identify BrdU$^+$ cells; number above bracketed line (left) indicates percent BrdU$^+$ cells (mean ± s.d.). (**b**) Frequency of CD27$^+$ or CD27$^-$ BrdU$^+$ 2W1S:I-A^{b+} CD4$^+$ memory T cells, based on the gates in **a**. Each symbol represents an individual mouse; small horizontal lines indicate the mean. $^*P = 0.03$, intravenous sample, $^{**}P = 0.002$, intranasal sample (paired two-tailed Student's *t*-test). (**c**) Expression of CD122 and CD27 on 2W1S:I-A^{b+} CD4$^+$ memory T cells induced by intravenous infection. Numbers in quadrants indicate percent CD122$^+$CD27$^-$ cells (top left) cells or CD122$^+$CD27$^+$ cells (top right; mean ± s.d. of five mice). (**d**) Frequency of BrdU$^+$ 2W1S:I-A^{b+} CD4$^+$ memory cells (left) in mice left uninjected (circles) or injected with IL-15–IL-15Rα complexes (triangles) and given BrdU for 5 d beginning 20 d after intravenous infection with LM-2W1S, identified as described in **a**. Each symbol represents an individual mouse; small horizontal lines indicate the mean. Middle and right, BrdU incorporation by CD27$^+$ (solid lines) or CD27$^-$ (gray-filled histograms) 2W1S:I-A^{b+} CD4$^+$ memory T cells in mice left uninjected (middle) or injected with IL-15–IL-15Rα complexes (right) and given BrdU for 5 d beginning 20 d after intravenous infection with LM-2W1S. $^*P = 0.003$, IL-15–IL-15Rα complex versus untreated (unpaired two-tailed Student's *t*-test). Data are representative of three (**a**,**b**), two (**c**) or one (**d**) experiment(s).

indicate that a lack of IL-15R expression limits the homeostatic proliferation of CD27$^-$ CD4$^+$ memory T cells.

DISCUSSION

Here we found that intravenous or intranasal infection with LM-2W1S induced polyclonal 2W1S:I-A^b–specific CD4$^+$ memory T cells. The emergence of memory-phenotype cells was preceded by robust proliferation of naive cells, which peaked in the secondary lymphoid organs about a week after infection. In both infections, the number of 2W1S:I-A^b–specific CD4$^+$ T cells decreased rapidly after the peak. This contraction phase ended on day 20, after which the number of cells decreased slowly. The abrupt change in survival observed at day 20 indicated that this is when the memory phase of this response begins. Most of the 2W1S:I-A^b–specific CD4$^+$ T cells induced by intravenous infection were in the secondary lymphoid organs during the memory phase, with considerably fewer cells in the bone marrow. Thus, the secondary lymphoid organs are the main reservoir of endogenous polyclonal CD4$^+$ memory T cells induced by intravenous bacterial infection and the bone marrow is not, as described for TCR-transgenic memory cells induced by immunization with peptide plus adjuvant[35].

Our results suggest that some but not all aspects of the T_H1-or-T_H17 and T_{EM}-or-T_{CM} paradigms apply to all CD4$^+$ memory T cells. The IFN-γ-producing memory cells induced by the transient bacterial infection studied here resembled T_H1 and T_{EM} cells because of their immediate ability to produce IFN-γ but not IL-17A and lack of CCR7 expression[3]. Similarly, the IL-17A-producing cells induced by intranasal infection resembled T_H17 and T_{EM} cells because of their immediate ability to produce IL-17A but not IFN-γ. However, these cells expressed CCR7 and thus were phenotypically similar to T_{CM} cells and were short-lived. In addition, the dominant population of memory cells induced by either infection route did not produce IFN-γ, IL-17A or IL-5 and was heterogeneous in terms of expression of CCR7 and CD27. Therefore, these cells did not fit easily into the T_H1, T_H2 and T_H17 paradigm or T_{CM} and T_{EM} paradigm. These cells may be less differentiated and thus able to become T_H1, T_H2 or T_H17 cells after secondary infection. Alternatively, these cells could be highly differentiated cells that produce lymphokines other than those that define the classical subsets.

The tendency of different routes of infection to induce different memory cells may be related to the innate cytokine environments of the relevant secondary lymphoid organs. Anatomic constraints make it likely that naive CD4$^+$ T cells first become activated in the nasal-associated mucosal lymphoid tissue after intranasal infection[28]. A published study has found that IL-17A-producing CD4$^+$ effector T cells are 'preferentially' induced in mice exposed to *Francisella tularensis* organisms via the respiratory mucosa[26]. Similarly, another study has shown that infection of the upper airway with *Streptococcus pneumoniae* organisms generates a population of IL-17A-producing CD4$^+$ T cells[27]. Thus, it is possible that the environment in mucosal secondary lymphoid organs is especially conducive to the differentiation of IL-17A-producing T cells. As IL-6 is required for the differentiation of these cells[36,37], it is noteworthy that dendritic cells from the intestinal mucosal tissue have been reported to be better IL-6 producers than are splenic dendritic cells[38]. In addition, transforming growth factor-β, which is also essential for the differentiation of IL-17A-producing T cells, is abundant in the mucosal tissues[39]. Conversely, splenic dendritic cells are potent producers of IL-12 (ref. 40), which is required for the differentiation of IFN-γ-producing T cells[41].

Our results confirm the idea that the number of CD4$^+$ memory T cells decreases slowly over time, at least in some cases. Published work has reported this finding for IFN-γ-producing CD4$^+$ memory T cells induced by infection with lymphocytic choriomeningitis virus[42]. We also found that the total population of 2W1S:I-A^b–specific CD4$^+$ memory T cells induced by intravenous bacterial infection, including those with IFN-γ-production potential, decreased slowly, with a half-life of about 40 d, between days 20 and 250 of the memory phase. It is worth noting that the aforementioned viral infection[42] and the bacterial infections studied here were cleared very quickly from the host. Thus, the decrease in the number of CD4$^+$ memory T cells described in both cases may be related to a lack of persistent antigen presentation. It will be of interest to determine if the number of CD4$^+$ memory T cells also decreases during persistent infection caused by organisms such as *Salmonella enterica* serovar Typhimurium[43].

After day 250, the number of 2W1S:I-A^b–specific memory cells stabilized at a number only about twice the number of naive cells. This survival pattern was similar to that observed for polyclonal naive

© 2010 Nature America, Inc. All rights reserved.

T cells[12]. Thus, it is possible that many CD4$^+$ memory T cells do not live longer than their already long-lived naive precursors.

The decrease in the number of CD4$^+$ memory T cells induced by transient infection is in contrast to the considerable numerical stability of CD8$^+$ memory T cells[42]. As IL-15 is important for the homeostatic proliferation of both types of memory cells[44], it may be telling that most CD4$^+$ memory T cells induced by bacterial infection, especially those lacking CD27, did not express IL-15R. It is therefore reasonable to suspect that a low rate of IL-15-driven homeostatic proliferation contributed to the numerical decrease in CD4$^+$ memory T cell populations observed in our experiments. Our finding that increasing the availability of IL-15 in the form of IL-15–IL-15Rα complexes increased the homeostatic proliferation of CD4$^+$ memory T cells is consistent with this possibility.

IL-17A-producing effector cells did not efficiently enter the memory cell pool. One possible explanation for this finding is that these cells simply lost the ability to produce IL-17A[37]. Alternatively, the IL-17A-producing cells could have died because of a lack of CD27. CD27-CD70 interactions have been shown to be important for the maintenance of CD8$^+$ memory cells[31,45], perhaps via CD27 signaling through the adaptor TRAF5 (ref. 46). The lack of a CD27 signal may have also lead to lower expression of the antiapoptotic protein Bcl-2 and a greater rate of apoptosis than that of CD27$^+$ CD4$^+$ memory cells. In contrast, IFN-γ-producing memory cells may gain a survival benefit from the expression of T-bet, which has been reported to control CD122 expression and thus the capacity for IL-15-dependent homeostatic proliferation[47]. Challenging this scenario is the finding that T-bet expression is a marker of terminal differentiation and death in CD8$^+$ memory T cells[48].

Our results also demonstrated an association between CD27 expression and lymphokine-production potential. This finding adds to other evidence indicating that signaling through CD27 is causally related to the acquisition of IFN-γ-production potential[49,50], perhaps by contributing to the induction of T-bet[51]. However, it is worth noting that about half of the RORγt$^+$ 2W1S:I-A^b–specific memory cells induced by intranasal infection expressed CD27 but did not produce IFN-γ or IL-17A and could have been committed to the production of IL-22 or IL-17F[52]. Thus, CD27 may be necessary but not sufficient for IFN-γ production by CD4$^+$ memory cells and may be not permissive for IL-17A production. This possibility is supported by work indicating that CD27$^+$ γδ T cells cannot become IL-17-producing cells[53].

Finally, our results have implications for protective immunity. Intranasal immunization of mice with *S. pneumoniae* induces protective immunity that is dependent on IL-17A and CD4$^+$ T cells[54]. Our findings suggest that this immunity may be short-lived, because IL-17A-producing CD4$^+$ effector T cells do not survive to become memory cells. In support of this suggestion is the clinical observation that streptococcal infections such as otitis media tend to recur[55].

METHODS

Methods and any associated references are available in the online version of the paper at http://www.nature.com/natureimmunology/.

Accession codes. UCSD-Nature Signaling Gateway (http://www.signaling-gateway.org): A000630 and A000546.

ACKNOWLEDGMENTS

We thank S. Jameson, H. Chu and J. Taylor for reviewing the manuscript; J. Walter, J. McLachlan and A. Schmidt for technical assistance; and P. Champoux and N. Shah for flow cytometry sorting. Supported by the US National Institutes of Health (AI39614, AI66016 and AI27998 to M.K.J.; T32-AI07313 to A.J.P.; and T32-CA9138 to M.P.).

AUTHOR CONTRIBUTIONS

M.P. designed the study, did experiments, analyzed data and wrote the manuscript; J.L.L., A.J.P., T.Z. and T.D. did experiments; P.P.C. designed experiments; and M.K.J. designed the study, analyzed data and wrote the manuscript.

Published online at http://www.nature.com/natureimmunology/.
Reprints and permissions information is available online at http://npg.nature.com/reprintsandpermissions/.

© 2010 Nature America, Inc. All rights reserved.

1. Jenkins, M.K. *et al.* In vivo activation of antigen-specific CD4 T cells. *Annu. Rev. Immunol.* **19**, 23–45 (2001).
2. Ahmed, R. & Gray, D. Immunological memory and protective immunity: understanding their relation. *Science* **272**, 54–60 (1996).
3. Sallusto, F., Lenig, D., Forster, R., Lipp, M. & Lanzavecchia, A. Two subsets of memory T lymphocytes with distinct homing potentials and effector functions. *Nature* **401**, 708–712 (1999).
4. Masopust, D., Vezys, V., Marzo, A.L. & Lefrancois, L. Preferential localization of effector memory cells in nonlymphoid tissue. *Science* **291**, 2413–2417 (2001).
5. Reinhardt, R.L., Khoruts, A., Merica, R., Zell, T. & Jenkins, M.K. Visualizing the generation of memory CD4 T cells in the whole body. *Nature* **410**, 101–105 (2001).
6. Seder, R.A. & Ahmed, R. Similarities and differences in CD4$^+$ and CD8$^+$ effector and memory T cell generation. *Nat. Immunol.* **4**, 835–842 (2003).
7. Zhou, L., Chong, M.M. & Littman, D.R. Plasticity of CD4$^+$ T cell lineage differentiation. *Immunity* **30**, 646–655 (2009).
8. Reiner, S.L. & Locksley, R.M. The regulation of immunity to *Leishmania major*. *Annu. Rev. Immunol.* **13**, 151–177 (1995).
9. Swain, S.L., Hu, H. & Huston, G. Class II-independent generation of CD4 memory T cells from effectors. *Science* **286**, 1381–1383 (1999).
10. Lohning, M. *et al.* Long-lived virus-reactive memory T cells generated from purified cytokine-secreting T helper type 1 and type 2 effectors. *J. Exp. Med.* **205**, 53–61 (2008).
11. Li, J., Huston, G. & Swain, S.L. IL-7 promotes the transition of CD4 effectors to persistent memory cells. *J. Exp. Med.* **198**, 1807–1815 (2003).
12. Hataye, J., Moon, J.J., Khoruts, A., Reilly, C. & Jenkins, M.K. Naive and memory CD4$^+$ T cell survival controlled by clonal abundance. *Science* **312**, 114–116 (2006).
13. Marzo, A.L. *et al.* Initial T cell frequency dictates memory CD8$^+$ T cell lineage commitment. *Nat. Immunol.* **6**, 793–799 (2005).
14. Badovinac, V.P., Haring, J.S. & Harty, J.T. Initial T cell receptor transgenic cell precursor frequency dictates critical aspects of the CD8$^+$ T cell response to infection. *Immunity* **26**, 827–841 (2007).
15. Rees, W. *et al.* An inverse relationship between T cell receptor affinity and antigen dose during CD4$^+$ T cell responses in vivo and in vitro. *Proc. Natl. Acad. Sci. USA* **96**, 9781–9786 (1999).
16. Moon, J.J. *et al.* Naive CD4$^+$ T cell frequency varies for different epitopes and predicts repertoire diversity and response magnitude. *Immunity* **27**, 203–213 (2007).
17. Ertelt, J.M. *et al.* Selective priming and expansion of antigen-specific Foxp3$^-$ CD4$^+$ T cells during *Listeria monocytogenes* infection. *J. Immunol.* **182**, 3032–3038 (2009).
18. Muller, W.J. *et al.* Recombinant *Listeria monocytogenes* expressing an immunodominant peptide fails to protect after intravaginal challenge with herpes simplex virus-2. *Arch. Virol.* **153**, 1165–1169 (2008).
19. Portnoy, D.A., Auerbuch, V. & Glomski, I.J. The cell biology of *Listeria monocytogenes* infection: the intersection of bacterial pathogenesis and cell-mediated immunity. *J. Cell Biol.* **158**, 409–414 (2002).
20. Moon, J.J. *et al.* Tracking epitope-specific T cells. *Nat. Protoc.* **4**, 565–581 (2009).
21. Kaech, S.M., Hemby, S., Kersh, E. & Ahmed, R. Molecular and functional profiling of memory CD8 T cell differentiation. *Cell* **111**, 837–851 (2002).
22. Khoruts, A., Mondino, A., Pape, K.A., Reiner, S.L. & Jenkins, M.K. A natural immunological adjuvant enhances T cell clonal expansion through a CD28-dependent, interleukin (IL)-2-independent mechanism. *J. Exp. Med.* **187**, 225–236 (1998).
23. Pape, K.A., Merica, R., Mondino, A., Khoruts, A. & Jenkins, M.K. Direct evidence that functionally impaired CD4$^+$ T cells persist in vivo following induction of peripheral tolerance. *J. Immunol.* **160**, 4719–4729 (1998).
24. Szabo, S.J. *et al.* A novel transcription factor, T-bet, directs Th1 lineage commitment. *Cell* **100**, 655–669 (2000).
25. Ivanov, I.I. *et al.* The orphan nuclear receptor RORγt directs the differentiation program of proinflammatory IL-17$^+$ T helper cells. *Cell* **126**, 1121–1133 (2006).
26. Woolard, M.D., Hensley, L.L., Kawula, T.H. & Frelinger, J.A. Respiratory *Francisella tularensis* live vaccine strain infection induces Th17 cells and prostaglandin E_2, which inhibits generation of γ interferon-positive T cells. *Infect. Immun.* **76**, 2651–2659 (2008).
27. Zhang, Z., Clarke, T.B. & Weiser, J.N. Cellular effectors mediating Th17-dependent clearance of pneumococcal colonization in mice. *J. Clin. Invest.* **119**, 1899–1909 (2009).
28. Park, H.S. *et al.* Primary induction of CD4 T cell responses in nasal associated lymphoid tissue during group A streptococcal infection. *Eur. J. Immunol.* **34**, 2843–2853 (2004).

29. Hikono, H. *et al.* Activation phenotype, rather than central- or effector-memory phenotype, predicts the recall efficacy of memory CD8+ T cells. *J. Exp. Med.* **204**, 1625–1636 (2007).
30. Snyder, C.M. *et al.* Memory inflation during chronic viral infection is maintained by continuous production of short-lived, functional T cells. *Immunity* **29**, 650–659 (2008).
31. Hendriks, J. *et al.* CD27 is required for generation and long-term maintenance of T cell immunity. *Nat. Immunol.* **1**, 433–440 (2000).
32. Hendriks, J., Xiao, Y. & Borst, J. CD27 promotes survival of activated T cells and complements CD28 in generation and establishment of the effector T cell pool. *J. Exp. Med.* **198**, 1369–1380 (2003).
33. Dolfi, D.V. *et al.* Late signals from CD27 prevent Fas-dependent apoptosis of primary CD8+ T cells. *J. Immunol.* **180**, 2912–2921 (2008).
34. Rubinstein, M.P. *et al.* Converting IL-15 to a superagonist by binding to soluble IL-15Rα. *Proc. Natl. Acad. Sci. USA* **103**, 9166–9171 (2006).
35. Tokoyoda, K. *et al.* Professional memory CD4+ T lymphocytes preferentially reside and rest in the bone marrow. *Immunity* **30**, 721–730 (2009).
36. Weaver, C.T., Harrington, L.E., Mangan, P.R., Gavrieli, M. & Murphy, K.M. Th17: an effector CD4 T cell lineage with regulatory T cell ties. *Immunity* **24**, 677–688 (2006).
37. Korn, T., Bettelli, E., Oukka, M. & Kuchroo, V.K. IL-17 and Th17 cells. *Annu. Rev. Immunol.* **27**, 485–517 (2009).
38. Sato, A. *et al.* CD11b+ Peyer's patch dendritic cells secrete IL-6 and induce IgA secretion from naive B cells. *J. Immunol.* **171**, 3684–3690 (2003).
39. Kelsall, B. Recent progress in understanding the phenotype and function of intestinal dendritic cells and macrophages. *Mucosal Immunol.* **1**, 460–469 (2008).
40. Reis e Sousa, C. *et al.* In vivo microbial stimulation induces rapid CD40 ligand-independent production of interleukin 12 by dendritic cells and their redistribution to T cell areas. *J. Exp. Med.* **186**, 1819–1829 (1997).
41. Hsieh, C.S., Heimberger, A.B., Gold, J.S. & O'Garra, A. Development of T_H1 CD4+ T cells through IL-12 produced by *Listeria*-induced macrophages. *Science* **260**, 547–549 (1992).
42. Homann, D., Teyton, L. & Oldstone, M.B. Differential regulation of antiviral T-cell immunity results in stable CD8+ but declining CD4+ T-cell memory. *Nat. Med.* **7**, 913–919 (2001).
43. Monack, D.M., Mueller, A. & Falkow, S. Persistent bacterial infections: the interface of the pathogen and the host immune system. *Nat. Rev. Microbiol.* **2**, 747–765 (2004).
44. Surh, C.D. & Sprent, J. Homeostasis of naive and memory T cells. *Immunity* **29**, 848–862 (2008).
45. Allam, A. *et al.* The CD8+ memory T-cell state of readiness is actively maintained and reversible. *Blood* **114**, 2121–2130 (2009).
46. Kraus, Z.J., Haring, J.S. & Bishop, G.A. TNF receptor-associated factor 5 is required for optimal T cell expansion and survival in response to infection. *J. Immunol.* **181**, 7800–7809 (2008).
47. Intlekofer, A.M. *et al.* Effector and memory CD8+ T cell fate coupled by T-bet and eomesodermin. *Nat. Immunol.* **6**, 1236–1244 (2005).
48. Joshi, N.S. *et al.* Inflammation directs memory precursor and short-lived effector CD8+ T cell fates via the graded expression of T-bet transcription factor. *Immunity* **27**, 281–295 (2007).
49. Soares, H. *et al.* A subset of dendritic cells induces CD4+ T cells to produce IFN-γ by an IL-12-independent but CD70-dependent mechanism in vivo. *J. Exp. Med.* **204**, 1095–1106 (2007).
50. Keller, A.M., Schildknecht, A., Xiao, Y., van den Broek, M. & Borst, J. Expression of costimulatory ligand CD70 on steady-state dendritic cells breaks CD8+ T cell tolerance and permits effective immunity. *Immunity* **29**, 934–946 (2008).
51. van Oosterwijk, M.F. *et al.* CD27–CD70 interactions sensitise naive CD4+ T cells for IL-12-induced T_h1 cell development. *Int. Immunol.* **19**, 713–718 (2007).
52. Yang, X.O. *et al.* T helper 17 lineage differentiation is programmed by orphan nuclear receptors RORα and RORγ. *Immunity* **28**, 29–39 (2008).
53. Ribot, J.C. *et al.* CD27 is a thymic determinant of the balance between interferon-γ- and interleukin 17-producing γδ T cell subsets. *Nat. Immunol.* **10**, 427–436 (2009).
54. Lu, Y.J. *et al.* Interleukin-17A mediates acquired immunity to pneumococcal colonization. *PLoS Pathog.* **4**, e1000159 (2008).
55. Yamanaka, N., Hotomi, M. & Billal, D.S. Clinical bacteriology and immunology in acute otitis media in children. *J. Infect. Chemother.* **14**, 180–187 (2008).

© 2010 Nature America, Inc. All rights reserved.

ONLINE METHODS

Mice. Six- to eight-week-old B6, B6.129S6-*Tbx21*^{tm1Glm}/J, B6.129P2(Cg)-*Rorc*^{tm2Litt}/J and B6.PL-Thy1^{a}/CyJ mice were from the Jackson Laboratory or the National Cancer Institute (B6). All mice were housed in specific pathogen–free conditions in accordance with guidelines of the University of Minnesota and National Institutes of Health. All animal experiments were approved by the Institutional Animal Care and Use Committee of the University of Minnesota.

***L. monocytogenes* infection.** Mice were injected intravenously (1×10^7 bacteria) or intranasally (1×10^7 bacteria) with *L. monocytogenes* expressing a recombinant protein consisting of chicken ovalbumin fused to the 2W1S peptide (EAWGALANWAVDSA)[17] or ESAT6 peptide[18]. In some experiments, mice were challenged intravenously after primary infection with 5×10^8 live LM-2W1S or LM-ESAT6. Challenged mice were killed 2 h later for analysis.

BrdU labeling. For analysis of homeostatic proliferation, mice were infected with LM-2W1S and at least 40 d later were given BrdU (0.8 mg/ml) in the drinking water for 12–14 d. In some cases, mice were injected intraperitoneally with complexes of recombinant mouse IL-15Rα–Fc chimera (7 μg per mouse) and recombinant mouse IL-15 (1.5 μg per mouse; both from R&D Systems) formed as described[34,56]. Mice were injected once a day for 2 d with IL-15–IL-15Rα complexes and BrdU (2 mg per mouse by intraperitoneal injection) and then BrdU was added to the drinking water (0.8 mg/ml) for an additional 3 d before spleens and lymph nodes were collected and stained as described below.

Tetramer production. Biotin-labeled soluble 2W1S:I-A^{b} molecules were produced and were expressed in *Drosophila melanogaster* S2 cells, then were purified and were made into tetramers with streptavidin-phycoerythrin or streptavidin-allophycocyanin (Prozyme) as described[16].

Tetramer enrichment and flow cytometry. Spleen and lymph node cells or leg bone marrow cells were prepared and then were stained for 1 h at 25 °C with 2W1S:I-A^{b}–streptavidin-phycoerythrin or 2W1S:I-A^{b}–streptavidin-allophycocyanin tetramer and peridinin chlorophyll protein–cyanine 5.5–conjugated antibody to CCR7 (anti-CCR7; 4B12; eBioscience) and then with anti-phycoerythrin and/or anti-allophycocyanin magnetic beads. Samples were then enriched for bead-bound cells on magnetized columns and a portion was removed for counting as described[16]. It was assumed that the leg bones contained one fifth of the bone marrow in the body[57]. The rest of the sample underwent surface staining on ice with Pacific Blue– or eFluor 450–conjugated anti-B220 (RA3-6B2; all antibodies from eBioscience unless otherwise noted), anti-CD11b (MI-70), anti-CD11c (N418) and anti-F4/80 (BM8; Caltag); Pacific Orange–conjugated anti-CD8α (5H10; Caltag); fluorescein isothiocyanate–conjugated anti-CD27 (LG.7F9); allophycocyanin–Alexa Fluor 750– or allophycocyanin–eFluor780–conjugated anti-CD4 (RM4-5); phycoerythrin-indotricarbocyanine–conjugated anti-CD3ε (145-2C11); phycoerythrin-conjugated anti-CD122 (5H4); and Alexa Fluor 700–conjugated anti-CD44 (IM7). For intracellular cytokine experiments, spleen and lymph node cells from challenged mice or *in vitro*–stimulated cultures containing phorbol 12-myristate 13-acetate (50 ng/ml), ionomycin (200 ng/ml) and brefeldin A (10 μg/ml; Sigma) underwent the tetramer enrichment and anti-CCR7 staining described above in buffer containing brefeldin A (10 μg/ml; Sigma) to prevent cytokine secretion. Surfaces of enriched cells were stained with combinations of antibodies listed above, then cells were treated with BD Cytofix/Cytoperm and stained with phycoerythrin-indotricarbocyanine–conjugated anti-IFN-γ (XMG1.2) or phycoerythrin-conjugated anti-IL-17A (TC11-18H10; BD Pharmingen). In some experiments, surfaces of enriched cells were stained, then cells were treated with Foxp3 Fixation/Permeabilization Concentrate and Diluent (eBioscience) and stained with phycoerythrin-conjugated anti-T-bet (eBio 4B10) or phycoerythrin-conjugated anti-RORγt (AFKJS-9), or they were treated with BD Cytofix/Cytoperm and stained with phycoerythrin-conjugated anti-Bcl-2 (3F11; BD Pharmingen). For BrdU labeling, surfaces of enriched cells were stained and incorporated BrdU was detected with a BrdU Flow kit according to the manufacturer's specifications (BD Pharmingen). In all cases, cells were then analyzed on an LSR II (Becton Dickinson). Data were analyzed with FlowJo software (TreeStar).

Memory cell transfer. Spleens and lymph nodes were collected from B6 mice infected at least 20 d earlier with LM-2W1S. For transfer of CD27^{-} cells, samples were depleted of CD27^{+} cells (95–97% purity) with biotin-conjugated anti-CD27, anti-biotin beads (Miltenyi) and LD columns (Miltenyi). For transfer of CD27^{+} cells, samples were enriched for CD4^{+} memory cells by the addition of biotin-conjugated anti-CD45RB (0.1 μg/ml) to the biotin-labeled antibody 'cocktail' provided in the Miltenyi CD4 Isolation kit, followed by the removal of biotin-labeled cells on an LS column. The remaining cells were stained with fluorochrome-labeled anti-CD44 and anti-CD27 before sorting of CD44^{+}CD27^{+} events with a FACSAria (Becton Dickinson). Purified cells were injected intravenously into B6.PL-Thy-1^{a} recipients. Then, 1 d or 14 d later, spleen and lymph node cells from the recipients were collected, were stained for 1 h at 25 °C for 2W1S:I-A^{b}–streptavidin–allophycocyanin tetramer and peridinin chlorophyll protein–cyanine 5.5–conjugated anti-CCR7 (4B12), then with phycoerythrin-conjugated anti-CD90.2 (53-2.1) and anti-phycoerythrin magnetic beads. Bead-bound cells were then stained with the non–T lineage–specific antibodies listed above (anti-CD8α, anti-CD4, anti-CD27 and anti-CD44) and cells were then analyzed on an LSR II (Becton Dickinson). Data were analyzed with FlowJo software (TreeStar).

Statistical analysis. Differences between data sets were analyzed by a paired or unpaired two-tailed Student's *t*-test. In **Figure 3**, a two-way analysis of variance with a Bonferroni's post-test was used to determine significance.

56. Stoklasek, T.A., Schluns, K.S. & Lefrancois, L. Combined IL-15/IL-15Ralpha immunotherapy maximizes IL-15 activity *in vivo*. *J. Immunol.* **177**, 6072–6080 (2006).
57. Boggs, D.R. The total marrow mass of the mouse: a simplified method of measurement. *Am. J. Hematol.* **16**, 277–286 (1984).

© 2010 Nature America, Inc. All rights reserved.

doi:10.1038/ni.1826